Surface-layer phase transitions in nematic liquid crystals

Natasha Kothekar and D. W. Allender
Department of Physics and Liquid Crystal Institute, Kent State University, Kent, Ohio 44242

R. M. Hornreich
Physics of Complex Systems, Weizmann Institute of Science, 76100 Rehovot, Israel

(Received 7 September 1993)

Surface-layer transitions in nematogenic materials characterized by a preferential planar surface interaction linear in the order parameter have been studied theoretically at temperatures above the bulk transition (T_{NI}). The coupled Euler-Lagrange nonlinear differential equations obtained from the Landau–de Gennes free energy were solved exactly by numerical integration. This problem had been studied previously employing various limits and approximations with several differences in the phase diagram reported. The exact results allow one to determine which of these differences are artifacts of the approximations used and which are dependent upon the ratio of elastic constants. It is found, for physically relevant elastic constants, that there is always a uniaxially ordered surface layer at sufficiently high temperatures. For weak surface coupling, no surface phase transition occurs and the uniaxial layer remains the stable state until T_{NI} is reached. When the surface coupling is increased, there is a single first-order (prewetting) transition from uniaxial to biaxial surface ordering as the temperature is reduced towards T_{NI}. This transition boundary becomes second order (by way of a tricritical point) when the surface coupling is further increased. We also find that the mean-field boundary is suppressed due to Berezinskii-Kosterlitz-Thouless (BKT)–type phase fluctuations. Also, these fluctuations can result in the re-entrant (with increasing surface coupling strength) uniaxial-biaxial phase boundary terminating on the bulk transition line rather than becoming asymptotic to it.

PACS number(s): 61.30.Gd, 64.70.Md, 68.45.Gd

The development of orientational order near surfaces and interfaces in nematogenic materials has been the focus of theoretical and experimental investigation for the past two decades. Most of these studies concentrated on the effect of homeotropic or homogeneous alignment of molecules at the surface [1–7]. As first suggested by Sheng [4], such alignment can lead to a prewetting phase transition in the boundary layer at a temperature above and separate from the bulk nematic-isotropic transition. For intermediate surface coupling, this prewetting transition line ends in a critical point in the interaction strength-temperature plane. More recently, it has been suggested that, for an unrubbed polymer coated substrate with no preferred direction in the plane of the surface, the molecules of the nematic liquid crystal may lie perpendicular to the substrate normal, resulting in a uniaxial surface layer with negative orientational order at temperatures well above the bulk nematic-isotropic phase transition (T_{NI}) [8]. This type of ordering leads to the possibility of two-dimensional transitions from a uniaxial to a biaxial surface layer when the surface coupling exceeds a critical value in the interaction strength-temperature plane.

Surface alignment at temperatures above the bulk nematic-isotropic transition on systems characterized by planar boundary conditions was first studied by Sluckin and Poniewierski [8], who considered a surface interaction linear in the order parameter and minimized the Landau-de Gennes free energy expression. Because the minimization equations cannot be solved analytically for arbitrary values of the elastic constants, they considered a limiting case in which one of the two symmetry-allowed elastic constants vanishes. The resulting phase diagram in the interaction strength (v) -temperature (t) plane [8,9] can then be divided into four distinct regions [see Fig. 1(a)]. For extremely weak surface coupling (region 1; $0<v<v_1$), only a uniaxially ordered surface layer exists for $T>T_{NI}$. For slightly larger interaction strength (region 2; $v_1<v<v_2$), there is a first-order transition from a uniaxial to a biaxial surface layer as the temperature is lowered towards T_{NI}. This prewetting line meets the bulk phase boundary at v_1, which divides regions 1 and 2. For intermediate surface coupling (region 3; $v_2<v<v_3$), there is first a continuous (second-order) transition from the uniaxial to an ordered biaxial layer as the temperature is decreased. As the temperature is further reduced, there is a first-order transition with no change in symmetry from this ordered biaxial layer. This first order boundary between the two ordered biaxial phases ends in a critical point. Finally when the surface coupling is increased beyond the critical point (region 4; $v>v_3$), there is only a continuous transition from the uniaxial to the biaxial surface layer. These results were later confirmed by Sheng *et al.* [10], who considered this problem more generally using the same limiting condition.

L'vov, Hornreich, and Allender [11] considered the same physical model but allowed the elastic constants to take arbitrary values. Since this made it impossible to analytically solve the minimization equations, an approx-

 ©1994 The American Physical Society

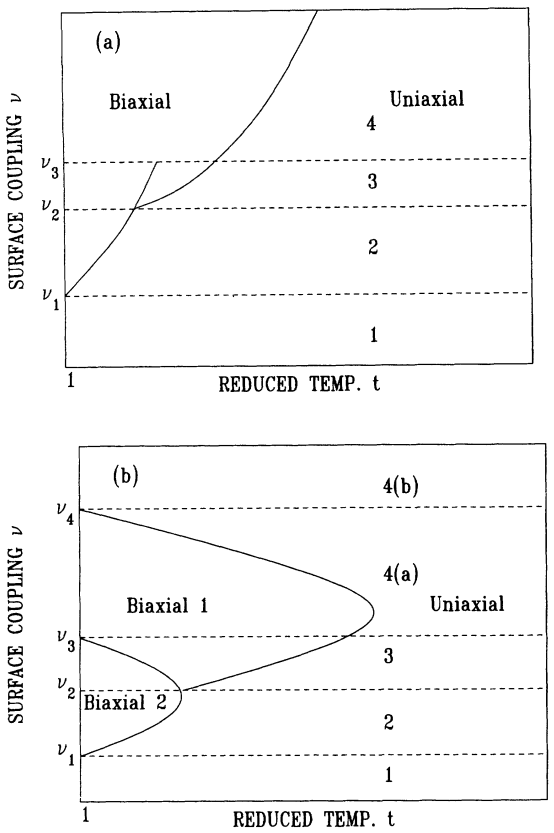

FIG. 1. Schematic versions of phase diagrams given in (a) [8], (b) [11], defining regions 1–4 in the surface interaction strength (ν) -temperature (t) plane. See text for details.

imate approach (known as the Ritz procedure), based upon using a trial function for the biaxial order parameter, was used. Their trial function had two free parameters, which were determined by minimizing the free energy. Although their phase diagram (in the interaction strength-temperature plane) has features in common with that of Sluckin and Poniewierski, there are some differences [see Fig. 1(b)]. Regions 1 and 2 are the same as in Ref. [8]. For intermediate surface coupling (region 3), they find a continuous transition from uniaxial to biaxial surface layer ordering and a biaxial-biaxial transition line which terminates on the T_{NI} boundary at ν_3 rather than at a critical point. However, due to the approximations used, they note that this line is suspect. Region 4(a) ($\nu_3<\nu<\nu_4$) of their phase diagram shows a continuous transition from the uniaxial to the biaxial surface layer, in agreement with [8]. However, this region has an upper bound (in ν) as the continuous transition line terminates on the T_{NI} boundary, thus giving rise to yet another region [4(b); $\nu>\nu_4$] in their phase diagram which, like region 1, has only a uniaxially ordered surface layer at temperatures above the bulk transition.

There is thus an open question as to whether the differences between the results of the two groups [8,11] are artifacts of the different approximations used or are really physical. To resolve this issue, we here reconsider the Landau-de Gennes free energy expression and find *exact* (albeit numerical) solutions to the problem which suffer from neither simplified variational equations nor approximate solution of the general equations.

We consider a semi-infinite nematic liquid crystal sample in the region $z>0$. The nematic tensor order parameter, in a principal axis system, can be written in appropriate reduced units [12] as

$$\mu_{ij}(\mathbf{r})=\frac{1}{\sqrt{6}}\begin{bmatrix}-\mu+\eta & 0 & 0\\ 0 & -\mu-\eta & 0\\ 0 & 0 & 2\mu\end{bmatrix}. \tag{1}$$

Within this formulation, the reduced bulk free energy is

$$f_b/A\xi=\int d\zeta\left[\frac{1}{4}t\mu^2+\frac{1}{12}t\eta^2-\mu^3+\mu\eta^2+\mu^4+\frac{2}{3}\mu^2\eta^2+\frac{1}{9}\eta^4+\frac{1}{4}\left[1+\frac{2}{3}\rho\right]\mu'^2+\frac{1}{12}\eta'^2\right]. \tag{2}$$

Here A is the area in the x-y plane, ξ is the correlation length, $\zeta=z/\xi$ and t is the scaled temperature [13]. The bulk nematic-isotropic transition occurs at $t=1$. The elastic constant ratio is ρ. In the Sluckin-Poniewierski approximation [8], our correlation length ξ goes to zero, which corresponds to taking the limit $\rho\to\infty$. Of course, the reduced units — e.g., ζ — must be appropriately rescaled in this limit.

The surface contribution to the free energy is assumed to be linear in the order parameter and is given by

$$f_s/A\xi=\nu\mu(0)\,, \tag{3}$$

where ν is proportional to the strength of the surface interaction. Planar boundary conditions are obtained by requiring $\nu\geq 0$.

The total free energy (f_b+f_s) is minimized when the Euler-Lagrange equations

$$\frac{1}{2}\left[1+\frac{2}{3}\rho\right]\mu''=\frac{t}{2}\mu-3\mu^2+\eta^2+4\mu^3+\frac{4}{3}\mu\eta^2\,,$$
$$\frac{1}{6}\eta''=\frac{1}{6}t\eta+2\mu\eta+\frac{4}{3}\mu^2\eta+\frac{4}{9}\eta^3\,, \tag{4}$$

subject to the boundary conditions

$$\mu'(0)=2\nu/\left[1+\frac{2}{3}\rho\right],\quad \eta'(0)=0\,, \tag{5}$$

$$\mu(\infty)\to 0,\quad \eta(\infty)\to 0\,, \tag{6}$$

are satisfied. The solution to these Euler-Lagrange equations can be obtained using a general purpose code (COLNEW), which solves mixed-order systems with multipoint boundary values [14]. The boundary condition at infinity can be simulated numerically by truncating ζ at a sufficiently large distance (take as $\zeta=b$). However, better numerical conditioning is achieved by constructing a boundary condition which annihilates those modes in the problem whose amplitude grows as ζ increases [15]. In fact, such a modification of the boundary conditions is

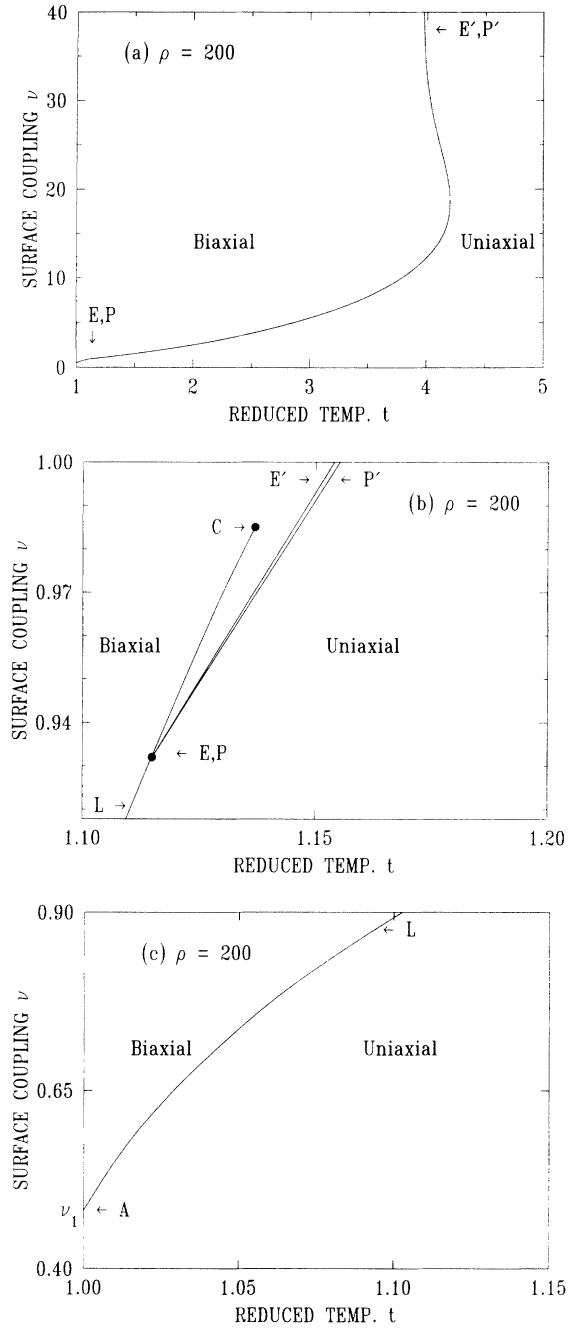

FIG. 2. (a) Phase diagram for $\rho=200$. Shown is the continuous (PP') transition boundary between the uniaxial and the biaxial surface layer, as obtained from a Landau (mean-field) formulation. Also shown is the BKT boundary (EE') between the two layers, which on this scale overlaps PP'. (b) An enlargement of region 3 (see Fig. 1) of part (a). With decreasing temperature, there is first a continuous transition (PP') from a uniaxial surface layer to a biaxial one. When the temperature is further reduced, there is a prewetting transition (PC) at which the biaxial surface layer goes into a more strongly ordered state. This prewetting line ends at a critical point (C). Finally, P denotes the critical end point and PL is the segment of the prewetting transition line separating regions of uniaxial and biaxial surface order. Also shown is the BKT line (EE'), which replaces the mean-field PP'. (c) An enlargement of regions 1 and 2 (see Fig. 1) of part (a), showing the prewetting line (AL) meeting the bulk transition line at $t=1$, $\nu=\nu_1$.

necessary in order to find solutions very close to $t=1$ or for large ρ's. In our case, the modified boundary conditions at infinity reduce to

$$\mu'(b)+\lambda_1\mu(b)=0\ ,$$
$$\eta'(b)+\lambda_2\eta(b)=0\ , \tag{7}$$

with

$$\lambda_1^2=t/(1+\tfrac{2}{3}\rho),\quad \lambda_2^2=t\ . \tag{8}$$

A common way of describing surface layer transitions is in terms of wetting [5,7,8,16], where the surface ordering is characterized by the parameters

$$\Gamma_\eta=\int_0^\infty \eta(\zeta)d\zeta,\quad \Gamma_\mu=-\int_0^\infty \mu(\zeta)d\zeta\ . \tag{9}$$

In our representation, a complete wetting transition corresponds to Γ_η and $\Gamma_\mu\to\infty$ as $T\to T_{NI}$. If, on the other hand, Γ_μ is finite and Γ_η is either finite or zero, the wetting is partial. A prewetting transition corresponds to a discontinuous jump in Γ_μ and Γ_η at a first-order transition above the bulk transition. We find that the uniaxial layer partially wets the surface at the bulk transition while the biaxial layer wets it completely.

The results of our calculations are summarized in Figs. 2–4. It is evident from these figures that the stability of

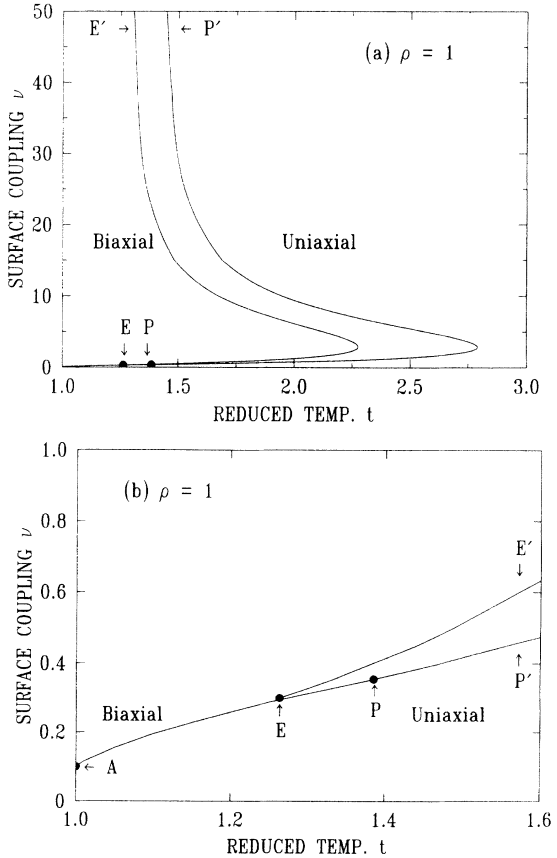

FIG. 3. (a) Phase diagram for $\rho=1$. The phase boundaries are as in Fig. 2(a). Here P and E denote the tricritical point, as obtained from the Landau theory and that of BKT, respectively. (b) An enlargement of the low interaction strength region of part (a), showing the tricritical point (P/E) and the intersection point ($t=1,\nu_1$).

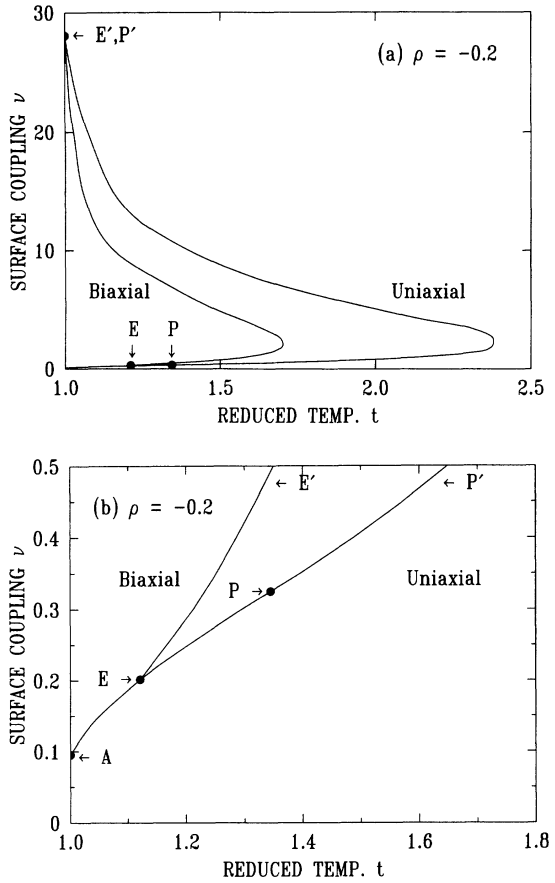

FIG. 4. (a) Phase diagram for $\rho=-0.2$. Here both the continuous transition line (PP') and the alternate BKT line (EE') intersect the bulk transition line, $t=1$. (b) An enlargement of the low interaction strength region of part (a).

the uniaxial or biaxial surface layer at temperatures above the bulk transition depends not only on the surface coupling (ν), but also strongly upon the elastic constant ratio (ρ). Figures 2(a), 3(a), and 4(a) are the phase diagrams for $\rho=200$, 1, and -0.2, respectively, and Figs. 2(b), 2(c), 3(b), and 4(b) are enlargements of the low surface interaction strength region of these graphs.

It is found, for large ρ's, that $\nu_4\rightarrow\infty$ [see Fig. 2(a)] and that the phase diagram has four regions [see Fig. 2(b)] similar to those found by Sluckin and Poniewierski [see Fig. 1(a)]. The prewetting transition line between the two biaxial surface layers in region 3 of the phase diagram ends in a critical point. As ρ is reduced from infinity, the prewetting line shortens and eventually disappears at $\rho\approx 103$. Therefore region 3 of the phase diagram disappears for $\rho\lesssim 103$ and, consequently, $\nu_2=\nu_3$. At $\rho\approx 103$, the critical point and the critical end point merge into a tricritical point. For $\rho\lesssim 103$, the continuous transition line meets the prewetting line in a tricritical point [see Figs. 3(b) and 4(b)] instead of the critical end point seen in Fig. 2.

The asymptotic part of the continuous phase boundary found when $\nu_4\rightarrow\infty$ shifts toward $t=1$ as ρ is decreased and finally intersects the bulk transition line at $\rho\approx -0.05$. Thus, for $\rho\lesssim -0.05$, the Landau theory result is that the uniaxial surface layer is the only stable ordered phase for $T>T_{NI}$ when $\nu>\nu_4$.

However, the continuous transition boundary determined from Landau theory, as noted by Sluckin and Poniewierski [8], is not the true thermodynamic boundary since the mean-field solution neglects fluctuations. Close to the transition boundary, the uniaxially ordered surface layer has the symmetry of the two-dimensional XY model. Long-wavelength in-plane phase fluctuations of the order parameter are therefore crucial, as shown by Berezinskii [17] and Kosterlitz and Thouless [18,19]. These BKT fluctuations lead to the suppression of the mean-field solution and result in a shift in the continuous phase boundary [11]. For our case, the fluctuations are characterized by an effective stiffness K_b, and the relevant fluctuation free energy is given by [11,20]

$$F_{\mathrm{BKT}}=\frac{1}{2}K_b\int d^2r(\nabla\theta)^2\ , \tag{10}$$

where θ is the in-plane angle between a local principal axis and the x axis. The effective stiffness K_b can be calculated directly from our numerical solution for the order parameter [11,20]. It then follows directly from the analysis of BKT that the critical temperature T_s is given by [21]

$$\lim_{T\rightarrow T_s^-}K_b=\frac{8}{\pi}k_bT_s\ , \tag{11}$$

where k_b is Boltzmann's constant.

The BKT boundaries are calculated for $T_s\approx 350$ K using typical parameter values [22]. These are the relevant continuous transitions for two-dimensional systems. As can be seen in the figures, the biaxial surface layer becomes unstable with respect to BKT-type phase fluctuations with increasing t before the mean-field phase boundary is reached. However, the gap between the mean-field and BKT phase boundaries decreases with increasing ρ and disappears entirely as $\rho\rightarrow\infty$ [see Fig. 2(a)]. We also find that the BKT line intersects the bulk transition line at $\rho\approx 0$. Since the BKT boundary is the relevant one, we see that region 4(b) in our phase diagram occurs, in fact, for $\rho\lesssim 0$ rather than $\rho\lesssim -0.05$.

A possible experimental method to detect the BKT phase boundary is evanescent-wave ellipsometry [23], which measures the phase difference Δ between p- and s-polarized radiation incident on the liquid-crystal–substrate interface and totally reflected at the critical angle. Since the biaxial state is birefringent in the film plane while the uniaxial one is not, this phase shift, which is proportional to the birefringence, will characterize the phase transition experimentally. However, this technique probes only singularities associated with static critical behavior, so confirmation of the transition's BKT character may be difficult. A better approach may therefore be to study the dynamics of the critical behavior by inelastic light scattering [20].

There has not been as yet any experimental confirmation of a biaxial surface layer above the bulk transition. This may be due to very weak surface coupling. Physical ρ values are generally between 0 and 1.

The values for the parameters in the free energy are obtained by using the standard expression [4].

$$F=\int dz[\,AS^2-BS^3+DS^4+L(dS/dz)^2+GS\delta(z)\,]\ . \tag{12}$$

In order to compare this expression with the uniaxial contributions to Eqs. (1) and (2) (i.e., $\eta=0$), we set $\mu=SD/B$, $\xi=Bz/2\sqrt{LD}$, $\nu=D^{3/2}G/2\sqrt{L}B^2$, and $f=(f_b+f_s)/A\xi=D^{5/2}F/2\sqrt{L}B^3$. Taking typical values [4,22] $B=0.53\times10^7$ ergs/cm^3, $D=0.98\times10^7$ ergs/cm^3, and $L=4.5\times10^{-7}$ ergs/cm, we obtain $G=2\sqrt{L}B^2\nu/D^{3/2}=1.2\nu$ ergs/cm^2. Thus, for $\nu=1.0$, which is in the theoretically interesting range, $G=1.2$ ergs/cm^2. Experimentally, G can either be measured directly or can be related to the anchoring energy W by the relationship $W=3G|S(0)|$. Birefringence data [24,25] on 4-cyano-4′-*n*-pentabiphenyl (5CB) gives $G\sim38$ ergs/cm^2 for a rubbed polyvinyl alcohol coated surface, but only 0.85 erg/cm^2 for an SiO film. Also, anchoring energies W have been found to range from 1 down to 10^{-4} erg/cm^2 [26]. Thus the predicted phase transitions should be observable as appropriate surface interaction potentials are attainable. However, we have only considered a surface interaction linear in the order parameter. Quadratic coupling could further increase the surface interaction strength needed to observe the BKT transition. Work is presently in progress to determine the effect of including quadratic as well as linear terms in the surface contribution to the free energy.

This work has been supported in part by the National Science Foundation under Science and Technology Center ALCOM DMR89-20147, and the Basic Research Foundation, admininistered by the Israeli Academy of Arts and Sciences, Jerusalem, Israel. We acknowledge helpful discussions with E. C. Gartland regarding the use of COLNEW.

[1] P. Sheng, Phys. Rev. Lett. **37**, 1059 (1976).
[2] K. Miyano, Phys. Rev. Lett. **43**, 51 (1979).
[3] D. W. Allender, G. L. Henderson, and D. L. Johnson, Phys. Rev. A **24**, 1086 (1981).
[4] P. Sheng, Phys. Rev. A **26**, 1610 (1982).
[5] M. M. Telo da Gama, Mol. Phys. **52**, 611 (1984).
[6] A. Mauger, G. Zribi, D. L. Mills, and John Toner, Phys. Rev. Lett. **53**, 2485 (1984).
[7] A. Poniewierski and T. J. Sluckin, Mol. Cryst. Liq. Cryst. **111**, 373 (1984).
[8] T. J. Sluckin and A. Poniewierski, Phys. Rev. Lett. **55**, 2907 (1985); and in *Fluid Interfacial Phenomena,* edited by C. A. Croxton (Wiley, New York, 1985), p. 215.
[9] In our notation, ν corresponds to h_1 in Ref. [8].
[10] P. Sheng, Bo-Zang Li, Minyao Zhou, Thomas Moses, and Y. R. Shen, Phys. Rev. A **46**, 946 (1992).
[11] Y. L'vov, R. M. Hornreich, and D. W. Allender, Phys. Rev. E **48**, 1115 (1993).
[12] The tensor order parameter is the same given in Eq. (10b) of [11]. Note that both representations given in [11] are completely equivalent and contain the entire set of solutions. Transformations from one representation to the other can be made by the following equations: $-\mu+\eta=2\mu_1$ and $2\mu=-\mu_1+\eta_1$.
[13] See Eqs. (1) and (12) of [11].
[14] U. Ascher, J. Chrstiansen, and R. D. Russell, ACM Trans. Math. Software **7**, 209 (1981).
[15] U. Ascher, R. M. M. Mattheij, and R. D. Russel, *Numerical Solution of Boundary Value Problems for Ordinary Differential Equations* (Prentice Hall, Englewood Cliffs, NJ, 1988), pp. 486–490.
[16] A. Poniewierski and T. J. Sluckin, Mol. Cryst. Liq. Cryst. **126**, 143 (1985).
[17] V. L. Berezinskii, Zh. Eksp. Teor. Fiz. **61**, 1144 (1971) [Sov. Phys. JETP **34**, 610 (1971)].
[18] J. M. Kosterlitz and D. J. Thouless, J. Phys. C **5**, 1224 (1972).
[19] J. M. Kosterlitz and D. J. Thouless, J. Phys. C **6**, 1181 (1973).
[20] R. M. Hornreich, E. I. Kats, and V. V. Lebedev, Phys. Rev. A **46**, 4935 (1992).
[21] D. L. Stein, Phys. Rev. B **18**, 2397 (1978).
[22] H. J. Coles, Mol. Cryst. Liq. Cryst. **49**, 67 (1978); also cited in [10].
[23] W. Chen, L. J. Martinez-Miranda, H. Hsiung, and Y. R. Shen, Phys. Rev. Lett. **62**, 1860 (1989).
[24] H. Yokoyama, J. Chem. Soc. Faraday Trans. 2 **84**, 1023 (1988).
[25] The values $g=4.0$ and 0.09 in Yokoyama's results correspond to $G=38$ and 0.85 erg/cm^2, respectively. See [4] for the definition of g.
[26] H. Yokoyama, Mol. Cryst. Liq. Cryst. **165**, 265 (1988).